



Variability of *Kappaphycus alvarezii* cultivation in South-Sulawesi (Indonesia) related to the monsoon shift: Water quality, growth and colour quantification

Laurent Barillé ^{a,*}, Iona L.R. Paterson ^{a,b}, Simon Oiry ^a, Agus Aris ^{c,f}, Elizabeth J. Cook-Cottier ^d, Nurjannah Nurdin ^{c,e}

^a Institut des Substances et Organismes de la Mer, ISOMer, Nantes Université, UR 2160, Nantes F-44000, France

^b Tritonia Scientific Ltd, Dunstaffnage Marine Laboratories, Dunbeg, Oban, Scotland PA37 1QA, UK

^c Research and Development Center for Marine, Coast, and Small Island, Hasanuddin University, Jl. Perintis Kemerdekaan km.10, Makassar 90245, Indonesia

^d Scottish Association for Marine Science, Scottish Marine Institute, Oban, Scotland PA37 1QA, UK

^e Marine Science Department, Marine Science and Fisheries Faculty, Hasanuddin University, Makassar 90245, Indonesia

^f Vocational Faculty, Hasanuddin University, Jl. Perintis Kemerdekaan km.10, Makassar 90245, Indonesia

ARTICLE INFO

Keywords:

Macroalgae

K. alvarezii

Seasonal variability

Ice-ice

Spectral reflectance

ABSTRACT

Kappaphycus alvarezii is a red eucheumatoid seaweed of high global economic significance due to its carrageenan content. Nevertheless, notable unexplained fluctuations in growth and production persist, exacerbated by limited data availability, while spatial and temporal factors remain unclear. This research aimed to characterise the variability of water quality, growth and thallus colouration of a green morphotype of *K. alvarezii* related to the monsoon shift in South Sulawesi, Indonesia. The experiment was conducted from July to November over contrasting dry and wet seasons. Three cultivation cycles of ca. 40 days were monitored: Cycle 1 (July/August), Cycle 2 (August/October), and Cycle 3 (October/November). The Southeast monsoon season (Cycles 1 and 2) was characterised by higher salinities, but lower temperatures and nutrients. During the wet Northwest monsoon season (Cycle 3), the water was hotter, with higher concentrations of nitrates and phosphates, but lower salinities. The highest growth rate at harvest of 5.0 % day⁻¹ was observed during Cycle 3. Fresh biomass production per m of the cultivation line was significantly higher for Cycle 3, 827.78 ± SD 101.50 g.m⁻¹ compared to Cycle 1 and 2, respectively 484.38 ± SD 11.27 g.m⁻¹ and 510 ± SD 25.69 g.m⁻¹. The higher growth during the West monsoon was likely due to the increase in nutrient concentrations brought by freshwater runoff, which coincided with higher rainfall. The spectral signature of the green morphotype was very similar to green macrophyte spectra with higher reflectance in the 500–600 nm wavelength region. A decrease in the greenness optical index at 550 nm was observed at the end of each cultivation cycle, with the thalli appearing darker. This study showed marked variations in growth rates, with significantly higher growth during the wet West monsoon, in conjunction with a higher risk of production loss due to the prevalence of ice-ice disease.

1. Introduction

Seaweeds contributed approximately 35 million tons of global aquaculture production in 2022, showing an 8 % yearly rise over the last decade (FAO, 2022). Since the 1950s, seaweed aquaculture has developed exponentially with an increased demand for its products providing income to over 6 million families living in rural coastal areas (Cottier-Cook et al., 2021). Currently, Asia dominates seaweed aquaculture production, with China accounting for ~60 % of the global

volume, followed by Indonesia with ~30 % (FAO, 2022). Red algae of the genera *Eucheuma* and *Kappaphycus* (collectively known as Eucheumatoids) are of high economic significance due to their carrageenan content (Ferdouse et al., 2018; Brakel et al., 2021). This high-quality compound possesses gelling, thickening, and stabilising properties, making it a valuable resource for the food industry (Neish et al., 2017). These species are farmed in tropical to warm temperate countries, particularly in Southeast Asia (Indonesia, the Philippines, Malaysia), the western Indian Ocean (Tanzania, Madagascar), the Pacific islands, and

* Corresponding author.

E-mail address: Laurent.Barille@univ-nantes.fr (L. Barillé).

South America (Brazil, Ecuador) (Hayashi et al., 2017). Indonesia is the leading global producer of *Eucheuma* and *Kappaphycus*, followed by the Philippines, Malaysia, and Tanzania (Rimmer et al., 2021). *K. alvarezii* cultivation was introduced to Indonesia from the Philippines in the late 1970s (Hurtado et al., 2014). South Sulawesi is the largest producing region, accounting for 35 % of production (Rimmer et al., 2021). Generally, eucheumatoid cultivation occurs in remote, coastal areas where environmental and biometric data are sparse (Setyawidati et al., 2017).

The prevalence of crop failure due to disease and pest outbreaks is a growing threat to eucheumatoid aquaculture worldwide (Hurtado et al., 2006; Largo et al., 1995a, b; Vairappan et al., 2008). *K. alvarezii* is reported as more susceptible to disease and epiphyte infestation compared to the less valuable species *Euchema denticulatum* (Ward et al., 2021). A major threat to *K. alvarezii* is the “ice-ice” disease, a complex syndromic disease, which causes a whitening of the thallus (Hayashi et al., 2010). Seaweeds infected with the ice-ice disease can also be infested with epiphytic filamentous algae (EFAs), which may also impact their colouration (Msuya and Porter, 2014; Kambey et al., 2021). Various color morphotypes of *K. alvarezii* also occur in response to different environmental conditions (Hayashi et al., 2010; Tan et al., 2017). All aspects relating to the colour of cultivated seaweeds can be observed and possibly quantified by optical methods used in remote sensing. These methods can identify light absorptions and reflections and quantify the colour, which is related to pigmentary composition (Douay et al., 2022). Stressed or diseased vegetation will display a distinct spectral signature directly corresponding to the effect (loss of colour) on pigments and/or thallus internal structure (Gitelson and Merzlyak, 1996). To our knowledge, optical methods have never been applied to quantify colour changes for *Kappaphycus* cultivation.

Epidemics of EFA have been associated with variations in abiotic factors, including seawater temperature, salinity, nutrient concentrations and photoperiod (Vairappan, 2006; Kambey et al., 2021). Similarly, the ice-ice disease develops following shifts in the abiotic factors mentioned, stressing seaweed, making them more susceptible to pathogens (Msuya and Porter, 2014; Brakel et al., 2021). Growth and biochemical composition are also related to environmental conditions (Neish, 2013; Ndwala et al., 2022). Large variations in seasonal and regional production have been observed, with different growth trends in farms only kilometers apart (Neish, 2013; Simatupang et al., 2021). Temperature and salinity were identified as strong drivers of the variability in production (Hurtado et al., 2017; Msuya and Porter, 2014; Ndwala et al., 2022). Seasonal environmental changes in water quality are strongly related to the monsoon regime in South Sulawesi (Ambo-Rappe and Moore, 2018). The shift from the favourable East monsoon dry season (April–October) to the West monsoon wet season (November–February) is a critical time for the farmers, as they can lose a full production cycle (Nurdin, pers. comm.). However, the consequence of this crucial transition period on *Kappaphycus* growth and health has not been investigated.

This study, therefore, aimed to characterise the variability of *K. alvarezii* cultivation related to the shift from the favourable East monsoon to the less favourable West monsoon season in South Sulawesi, Indonesia. Growth, water quality, and seaweed colouration (i.e., a proxy for health status) were monitored under commercial conditions. Three cultivation cycles of the green morphotype of *K. alvarezii* were analysed from July to November. This study took place in the context of climate change modifying ocean conditions, which can affect the growth and survival of farmed seaweed worldwide (FAO, 2024). These global changes can also affect the seasonality of monsoons in Southeast Asia (Loo et al., 2015). Indonesian seaweed production has decreased in the last decade (FAO, 2024), and seasonal variability is a concern for eucheumatoid aquaculture in South Sulawesi (Nuryartono et al., 2021). Farmers from this region identified the changing monsoon season as the major problem for seaweed cultivation (Zamroni and Yamao, 2011). Still, the link between environmental variables and growth remains

unclear.

2. Materials & methods

2.1. Study sites

This study was conducted at two seaweed cultivation sites in the Takalar Regency, Southwest Sulawesi, namely Malelaya ($5^{\circ}34'29.64''$ S, $119^{\circ}25'29.999''$ E) and Punaga ($5^{\circ}35'2.257''$ S, $119^{\circ}25'52.058''$ E), 1.5 km apart (Fig. 1). Two locations were used to work with a farmer using the green morphotype of *K. alvarezii* but the genetic variation amongst cultivars was not quantified. The field experiment was conducted in July–November 2021 covering the South-East monsoon season (July–September) and the North-West monsoon season (October–November). Both farm sites are situated above the substratum composed of sand, rubble corals, seagrass and seaweeds. They are located ~3 km South of an estuary in Binanga Palomppakang. There is a semidiurnal tidal regime with a maximal amplitude of 2 m. For the Malelaya site, the water depth ranged from 20 to 130 cm at low and high tide, respectively. For Punaga, the range was 45–155 cm. Using satellite data (NASA Physical Oceanography DAAC, <https://doi.org/10.5067/GHMDA-2PJ19> and Copernicus Marine Service, <https://marine.copernicus.eu/>), we checked that there was no statistical difference between the two sites during the experiment for three main variables that could be retrieved from MODIS and Sentinel 3 OLCI sensors: temperature, Suspended Particulate Matter and chlorophyll *a* concentration (Mann-Whitney, $p > 0.05$). Cultivation Cycles 1 & 3 were in Malelaya and Cycle 2 was in Punaga.

2.2. Cultivation method and cycle

The seaweed culture method used for this experiment was the long-line system. It consisted of several nylon lines of 25 m in length and 0.5 m to 1 m apart. Each nylon line held individual thalli of *K. alvarezii*. At the start of each cultivation cycle, the initial mean weight ranged between 26 and 29 g (fresh weight), with no statistical difference (ANOVA, $p = 0.08$). The thalli were attached at ca. 20–25 cm intervals. For each cycle, three lines were chosen randomly, and three replicates of *K. alvarezii* were selected randomly per line and tagged. For each cycle, a minimum of nine replicates of *K. alvarezii* were identified and tagged. For Cycle 3, three extra lines with three replicates per line were monitored to anticipate a possible loss of samples due to the ice-ice disease. Plastic buoys were attached to every 5 m of the line, and anchors were used to secure the infrastructure of the seabed. In the study area, the cultivation cycles are approximately 40 days for *K. alvarezii*, but farmers could harvest their crops earlier. In fact, at the end of Cycle 1, the farmer harvested the seaweed after 30 days. For each cycle, measurements were done every 10 days at t_0 , t_{10} , t_{20} , t_{30} , and t_{40} . The selected timescale encompassed a South-East monsoon season (Hereafter East monsoon) with less rainfall, but cooler sea surface temperature (Cycles 1 & 2) and a wet North-West monsoon season (hereafter West monsoon) with a higher sea surface temperature (Cycle 3). Cycle 1 was from the 3 July to the 3 August; Cycle 2 was from the 18 August to the 4 October and Cycle 3 was from the 15 October to the 23 November 2021.

2.3. Growth data and production rate

The growth was measured every ten days. Each sample was untied from the line and brought to the shore, where the fresh weight was obtained with a field scale after leaving the sample draining for ten minutes on soft tissue. Each sample was also measured for its spectral reflectance. It was then tied back to the line. The Specific Growth Rate (SGR, %·d⁻¹) was calculated as the percentage growth rate per day, SGR = $[100 (\ln W_t / \ln W_0)]/t$ with W_t = weight after t days, W_0 = initial weight, t = time in days. To calculate the production rate (g·m⁻²), the average initial fresh weight was subtracted from the final weight at the

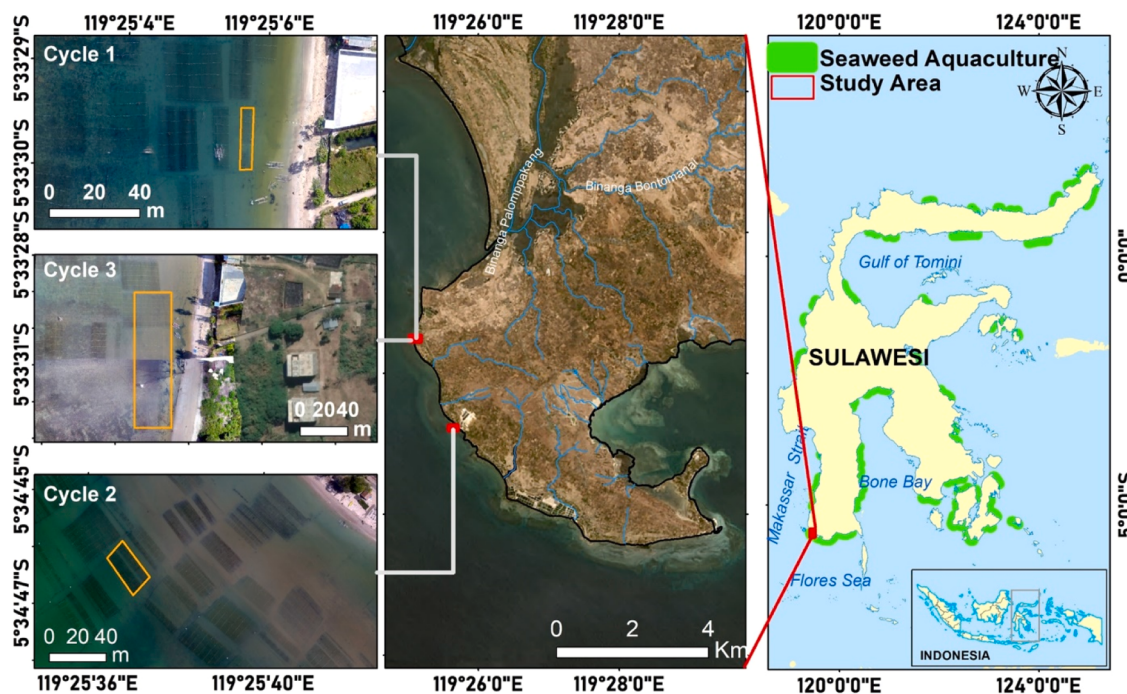


Fig. 1. Right panel - Coastal zones used for seaweed aquaculture in Sulawesi, Indonesia (green areas). The red square indicates the study area in the Takalar Regency. Centre panel - Location of the two study sites (red squares). River systems are represented in blue. Left panels - High-resolution drone images of the cultivation sites. Cycles 1 and 3 were located in Malelaya (northern site), and Cycle 2 was in Punaga (southern site). The yellow polygons denote the cultivation areas monitored for each cycle (1–3).

end of the cultivation cycle. The resulting weight (g) was then expressed per meter of cultivation line (m).

2.4. Spectral reflectance

Reflectance spectra of each *K. alvarezii* replicate were obtained using a field-portable Lamba NIR spectroradiometer, measuring the radiance expressed in SI units ($\text{mW cm}^{-2} \text{ nm}^{-2} \text{ sr}^{-1}$) between 400 and 1000 nm. After removing the dark current noise, the radiance of a 99 % reflective Spectralon® reference panel was measured to convert each radiance measurement into reflectance. Measurements were obtained using a fiberoptic cable. Mean reflectance was calculated from at least ten spectra replicates for each sample. Spectral responses in the visible-near infrared (VNIR) between 400 and 800 nm were observed, as this spectral range contains the absorption bands of photosynthetic and accessory pigments of *K. alvarezii* (Kumar et al., 2020) and it avoids the strong absorption by water in wavelengths higher than 800 nm. A moving average was applied with a 9 nm smoothing window to reduce the noise in the data. All spectra were standardized to reduce the effect of changes in light conditions (albedo variations) and to emphasize the spectral shapes in the visible range associated with the pigment composition (Douay et al., 2022). The Max-Min equation (Cao et al., 2017) was used:

$$R_{\lambda}^* = \frac{R_{\lambda} - \min(R_{\lambda})}{\max(R_{\lambda}) - \min(R_{\lambda})}$$

Where R_{λ} is the reflectance at each wavelength, and $\min(R_{\lambda})$ and $\max(R_{\lambda})$ corresponding to the minimum and maximum reflectance, respectively, in the same reflectance spectrum. The reflectance in the green (550 nm, R_{550}) was selected as a greenness optical index ranging from 0 to 1 to identify the change in seaweed colouration. This optical approach was also intended to detect signs of whitening due to the ice-ice disease. The methodology is detailed in Alevizos et al. (2024).

2.5. Environmental parameters

Seawater parameters were collected for each date of each cycle (t_0 , t_{10} , t_{20} , t_{30} , t_{40}). Salinity, temperature, pH and turbidity were measured *in situ* with six replicates randomly chosen in the cultivation plot. Water temperature, salinity and pH were measured using respectively a digital thermometer, a digital refractometer and a digital pH meter. Turbidity was measured with a turbidimeter and expressed in Nephelometric Turbidity Units (NTU). Three additional water samples were collected for nutrient analysis for each date of each cycle. The samples were stored in 1 L amber bottles and kept in a cool box during the process of transportation from the field to the laboratory. Total (dissolved) phosphorus and nitrogen were measured using a DREL 2800 spectrophotometer and processed corresponding to the methods described by Strickland and Parsons (1972). Depths were measured using a scaling pole. Current speed data (m.s^{-1}) were obtained at a coarse scale ($0.083^\circ \times 0.083^\circ$) for the Takalar Regency coastal area using the Global analysis forecast Copernicus product (https://data.marine.copernicus.eu/product/GLOBAL_ANALYSISFORECAST_PHY_001_024/description). At this scale, the data were used to characterise seasonal changes related to the monsoonal patterns with Westward vs. Eastward currents.

2.6. Statistical analysis

The normality and heteroscedasticity of data distributions were tested before each analysis using Shapiro and Levene tests respectively. For each cycle, a non-parametric Friedman test for repeated measures was performed to test for differences in fresh weight and specific growth rates between sampling intervals. The *a posteriori* Wilcoxon pairwise test was then performed to compare paired data, identifying which sampling intervals were different from one another. The spectral reflectance of each replicate was used to calculate the average greenness index at t_0 and the harvest date (t_{30} or t_{40}). A two-sample non-parametric Wilcoxon repeated-measures test was used to assess the changes in the greenness index of replicates during the cycles. Kruskal-Wallis and Mann-Whitney

pairwise tests were used to compare the colour of the seedlings between cycles at t_0 (i.e. comparing the colour of the cultivars). Environmental data were compared between cycles with a Kruskall-Wallis non-parametric test followed by Mann-Whitney pairwise comparisons. A Principal Component Analysis (PCA) was applied to the environmental dataset, to analyse the seasonal variations between the different cycles. Data were normalised before performing the analysis. Spearman correlations were calculated between growth and the environmental variables. Statistical analyses were carried out using R (R Core Team, 2022), and PRIMER 7 V 7.0.21 software.

3. Results

3.1. Environmental data

Regarding the physical variables, there were significant differences in the average water temperature between cycles (Kruskal-Wallis, $p < 0.01$), with 29.6°C (SD 2.9°C) for Cycle 1, 27.8°C (SD 0.5°C) for Cycle 2 and 30.9°C (SD 1.1°C) for Cycle 3 (Table 1). Cycle 3 corresponding to the wet monsoon season, was significantly hotter than the two others monitored during the dry monsoon (Mann-Whitney pairwise, $p < 0.01$). There were also significant differences in the average salinities between cycles (Kruskal-Wallis, $p < 0.01$), with 33.7 (SD 0.5) for Cycle 1, 34.0 (SD 0.5) for Cycle 2 and 30.7 (SD 1.7) for Cycle 3 (Table 1). Cycle 3 of the rainy season had significantly lower salinity than the two others of the dry season (Mann-Whitney pairwise, $p < 0.01$). There was significant variability of mean turbidity within cycles (Table 1, Kruskal-Wallis, $p < 0.01$). However, there was also a significant difference between cycles (Kruskal-Wallis, $p < 0.01$), with Cycle 3 having a higher average (9.72 NTU, SD 3.58) than Cycle 1 (8.98 NTU, SD 3.10) and Cycle 2 (6.8 NTU, SD 3.5) (Mann-Whitney pairwise, $p < 0.01$). There were also differences in the chemical variables. The average pH of Cycle 3 (7.32 SD 0.11) of the wet monsoon season was significantly lower than the two other cycles of the dry monsoon season, respectively Cycle 1 (7.66 SD 0.17) and Cycle 2 (7.64 SD 0.17) (Mann-Whitney pairwise, $p < 0.01$). Both nitrate and phosphate concentrations were highest during the wet monsoon season of Cycle 3 (Table 1). There were significant differences in the average water nitrate concentration between cycles (Kruskal-Wallis, $p < 0.01$), with Cycle 3 having a significantly higher concentration (0.09 mg.L^{-1} SD 0.03) than the two others (0.06 mg.L^{-1} SD 0.03) (Mann-Whitney pairwise, $p < 0.01$). The average phosphate concentration of Cycle 3 was significantly higher than that of Cycle 2 (Mann-Whitney pairwise, $p < 0.01$), but there was no difference with Cycle 1 (Mann-Whitney pairwise, $p = 0.76$). However, the highest concentrations were observed for the two last sampling dates of Cycle 3, t_{30} and t_{40} , with 0.06 mg.L^{-1} (SD 0.03) (Table 1). A PCA was applied to the environmental dataset to analyse the seasonal variations between the three cycles (Fig. 2). The first and the second principal components

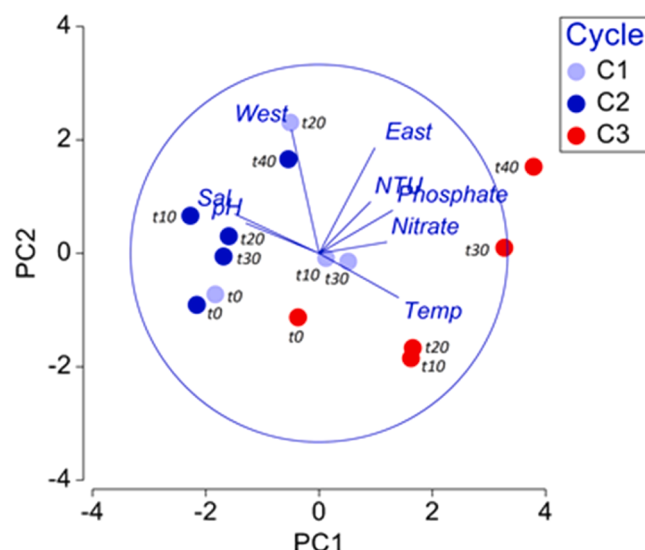


Fig. 2. Principal Component Analysis (PCA) plot with dates (Symbols & texts) and environmental variables (Vectors and blue text) for three cultivation cycles of *K. alvarezii* in South Sulawesi (Indonesia) covering the East and West monsoon period. West = Westward current, East = Eastward current, Sal = salinity, Temp = temperature, NTU = Nephelometric Turbidity Units.

accounted for 67 % of the total variance. There was a clear separation opposing the first two cycles corresponding to the East dry monsoon season and Cycle 3 corresponding to the West wet monsoon season. The first date of cycle 3 ($t_0 = 15$ th October 2021) is positioned in between cycles 1, 2 and the remaining sample dates ($t_{10}, t_{20}, t_{30}, t_{40}$) for cycle 3, suggesting that this date corresponds to the transition period between the East and West monsoon. The East monsoon period was characterized by Westward currents, high salinity and pH, but low temperature, nutrients and turbidity. Cycle 3 during the West monsoon was characterised by Eastward currents, higher temperature, nutrients and turbidity, but lower salinity and pH.

3.2. Seaweed colour change

The notable changes in the environmental conditions during Cycle 3 (wet season), corresponded with an incidence of ice-ice disease, when increased temperatures and lower salinity levels were recorded (Table 1). For Cycle 3 six replicates of *K. alvarezii* were lost after the t_{20} sampling date and two replicates were lost at t_{40} . There was no whitening of the remaining replicates, but partial discolouration of some thalli could be observed at the scale of the cultivation plot. However, the visually most conspicuous change at the end of cultivation Cycle 3 was a

Table 1

Environmental data (mean \pm SD) collected from July to November 2021 over three *Kappaphycus alvarezii* cultivation cycles in Takalar Regency (Indonesia) for temperature ($^\circ\text{C}$), salinity (PSU), nitrate (NO_3^-), phosphate (PO_4^{3-}), turbidity (NTU), pH, Eastward current (m.s^{-1}) and Westward current (m.s^{-1}).

Cycle	Day	Temp	Salinity	NO_3^-	PO_4^{3-}	NTU	pH	Current W	Current E
1	t_0	30.1 ± 0.3	33.8 ± 0.0	0.04 ± 0.02	0.02 ± 0.01	7.2 ± 1.4	7.9 ± 0.0	0.08	0.05
1	t_{10}	28.9 ± 0.3	33.0 ± 0.0	0.08 ± 0.03	0.04 ± 0.01	9.5 ± 2.8	7.7 ± 0.0	0.05	0.09
1	t_{20}	29.4 ± 0.5	34.1 ± 0.0	0.05 ± 0.02	0.03 ± 0.01	11.2 ± 4.0	7.5 ± 0.0	0.24	0.11
1	t_{30}	30.0 ± 0.2	33.9 ± 0.0	0.09 ± 0.03	0.05 ± 0.02	8.1 ± 1.8	7.5 ± 0.0	0.08	0.07
2	t_0	27.6 ± 0.2	34.0 ± 0.0	0.03 ± 0.01	0.02 ± 0.00	6.1 ± 1.1	7.6 ± 0.0	0.08	0.04
2	t_{10}	27.2 ± 0.2	34.2 ± 0.0	0.07 ± 0.01	0.02 ± 0.00	6.2 ± 1.1	7.7 ± 0.1	0.18	0.05
2	t_{20}	27.4 ± 0.1	33.8 ± 0.0	0.10 ± 0.01	0.03 ± 0.01	7.2 ± 4.5	7.8 ± 0.0	0.11	0.05
2	t_{30}	28.5 ± 0.0	34.3 ± 0.0	0.09 ± 0.03	0.02 ± 0.01	5.6 ± 2.9	7.6 ± 0.3	0.16	0.03
2	t_{40}	28.5 ± 0.1	34.2 ± 0.0	0.05 ± 0.01	0.02 ± 0.00	10.3 ± 3.7	7.6 ± 0.0	0.16	0.16
3	t_0	29.5 ± 0.4	34.2 ± 0.0	0.06 ± 0.01	0.02 ± 0.00	11.8 ± 1.7	7.5 ± 0.0	0.06	0.00
3	t_{10}	30.9 ± 0.3	29.9 ± 0.2	0.10 ± 0.02	0.02 ± 0.00	7.5 ± 0.6	7.2 ± 0.0	0.06	0.06
3	t_{20}	31.1 ± 0.5	29.9 ± 0.3	0.07 ± 0.01	0.03 ± 0.01	8.9 ± 2.6	7.2 ± 0.0	0.06	0.05
3	t_{30}	30.6 ± 0.2	29.8 ± 0.4	0.13 ± 0.03	0.06 ± 0.01	10.3 ± 5.5	7.4 ± 0.1	0.12	0.21
3	t_{40}	32.8 ± 0.6	30.0 ± 0.0	0.12 ± 0.03	0.06 ± 0.01	10.2 ± 3.9	7.3 ± 0.1	0.09	0.11

darkening of the thallus (Fig. 3). The reflectance spectra of *K. alvarezii* were characterized by a strong absorption in the visible range between 400 and 700 nm due to the presence of photosynthetic pigments, chlorophyll *a*, phycobiliproteins (Phycoerythrin and phycocyanin) and carotenoids (Fig. 4A). All spectra showed higher reflectance at 550 nm responsible for the green colour of the seaweed. A decrease in reflectance at 550 nm was associated with a darkening of the thallus which could be quantified (Fig. 4B). During the three cultivation cycles, the change in reflectance spectra of replicates and thus seaweed colour was observed between t_0 and the harvesting date (t_{30} , t_{40}). There was no statistical significance in the greenness index over Cycle 1 (Fig. 5A, Wilcoxon repeated-measures, $p > 0.05$), but it was significantly lower at the end of the culture for Cycle 2 (Fig. 5B, Wilcoxon repeated-measures, $p < 0.05$) and highly significantly lower for Cycle 3 during the wet season (Fig. 5C, Wilcoxon repeated-measures, $p < 0.01$). There was a significant variability of the greenness index between cycles (Kruskal-Wallis, $p < 0.01$). The cultivar used for Cycle 2 was significantly greener (higher greenness index at t_0) than the one used for Cycle 1 (Mann-Whitney pairwise, $p < 0.05$), which was itself not significantly different from the variant used in Cycle 3 (Mann-Whitney, $p > 0.05$). The lowest value of the greenness index was observed at the end of Cycle 3 (t_{40}) corresponding to darker *Kappaphycus* thalli with a low reflectance in the visible wavelength range (Fig. 5C).

3.3. Growth and production data

During the first cycle, the biomass (fresh weight) of *K. alvarezii* was significantly different between all dates (Friedman test & Wilcoxon pairwise $p < 0.05$, Fig. 6). The fresh weight increased linearly and reached more than four times its initial median weight over t_{30} , (25 g to 111.1 g). During the second cycle, the fresh weight increased between t_0 to t_{20} , but significantly decreased at t_{30} (102.2 ± 7.12 g at t_{20} vs. 86.67 ± 12.25 g at t_{30}) (Wilcoxon pairwise $p < 0.05$). From t_{30} to t_{40} , biomass increased significantly to 115 g (Wilcoxon pairwise $p < 0.05$). During Cycle 3, the biomass increased linearly over time, with each interval statistically significant (Friedman test & Wilcoxon pairwise $p < 0.05$). An increase in median fresh weight from 30 g to 195 g was observed. For the three cycles, there were significant differences in the Specific Growth Rate (SGR) between dates (Fig. 7, Friedman test, $p < 0.05$). During Cycle 1, the highest SGR was observed at t_{20} (Wilcoxon pairwise $p < 0.05$). At harvest (t_{30}), the SGR was $4.5\% \text{ day}^{-1}$. During Cycle 2, there was a significant decrease between t_{10} , t_{20} and t_{30} , t_{40} (Wilcoxon pairwise $p < 0.05$). SGR was $3.3\% \text{ day}^{-1}$ at harvest (t_{40}). During Cycle 3, there was a linear decrease of SGR from $6.6\% \text{ day}^{-1}$ at t_{10} to $5.0\% \text{ day}^{-1}$ at t_{40} . SGR showed a negative correlation with salinity and a positive correlation with phosphate concentration (Table 2). Salinity was negatively correlated with temperature and phosphate while

nutrients were positively correlated with turbidity. Significant differences were observed in the production (final weight of seaweed minus initial weight of seaweed) of *K. alvarezii* cultured during all cycles (Friedman Test, $p < 0.05$). Production over Cycle 1 (30-day cycle period) was $484.4 \pm \text{SD } 11.3 \text{ g.m}^{-1}$ and $510.0 \pm \text{SD } 25.7 \text{ g.m}^{-1}$ over Cycle 2 (40-day cycle period). The highest production was recorded during Cycle 3 (40-day cycle period) with $827.8 \pm \text{SD } 101.5 \text{ g.m}^{-1}$.

4. Discussion

Paradoxically, although seasonality is acknowledged as responsible for significant changes in growth, quality of carrageenan and ultimately, product sales (Hayashi et al., 2010, 2017; Kumar et al., 2014; Neish, 2013), causal relationships have not yet been clearly described. This work showed that the marked changes in water quality variables occurred during the wet West monsoon season in South Sulawesi compared to the dry East monsoon season and these were characterised by higher nutrient concentrations associated with higher growth. However, this season also had a higher risk of ice-ice disease, which leads to the whitening of the thallus. The changes in seaweed colour during the cultivation cycles, however, were quantified with a greenness spectral index showing a darkening of the thallus.

4.1. Seasonal changes in water quality

The cultivation area is in a tropical interocean exchange zone between the Pacific and Indian oceans (Gordon et al., 2019). The climatology is related to the functioning of the Indonesian throughflow within the Makassar Strait (Mayer and Damm, 2012), with strong seasonal changes in wind and current directions (Janßen et al., 2017). The East monsoon season (from April to September) is a dry period with Westward winds and currents. Eastward winds and currents and higher rainfall characterise the West monsoon season (from October to March). In a non-intuitive way, the water was cooler during the dry season. In this study, we observed the transition from the dry East monsoon, with higher salinity but lower temperature and nutrients, to the wet West monsoon, characterised by the opposite conditions. Interestingly, the PCA ordination also showed that higher nitrate and phosphate concentrations during the West monsoon season were also related to higher turbidity. The resuspension of nutrient-rich sediment can partly explain this higher nutrient concentration due to the eastward winds and currents. Likely, freshwater runoff would also contribute to higher nutrient levels, and the proximity to an estuary supports this hypothesis. During Cycle 3, the salinity also decreased to 29.8 coinciding with higher rainfall. The timing and intensity of rainfall are also related to the strength of the El Niño/La Niña Southern Oscillation with significant interannual variations (Hidayat et al., 2017; Setyawidati et al., 2017). Despite the seasonal variability, temperature, salinity and pH were all found to be in the optimum range for *K. alvarezii* growth (Aslan, 1998; Azanza and Ask, 2017; Hurtado et al., 2017; Kumar et al., 2020). Only the last sampling date of Cycle 3, when the average temperature of 32.8°C was recorded, could be described as in the upper limit range, where signs of stress can be expected (Kumar et al., 2020). The higher growth during the West monsoon was likely due to the increase in nutrient concentrations, even though we cannot exclude the genetic variations among the cultivars. Considering the range of temperature and salinity measured in this work, these variables were unlikely to interact with the nutrient uptake (Mandal et al., 2014). Hung et al. (2009) described a comparable seasonal pattern in Vietnam, with a higher growth during the wet monsoon attributed to an increase in inorganic nitrogen. Kotiya et al. (2011) similarly observed seasonal variations in nine coastal sites of India with higher growth of *K. alvarezii* corresponding to elevated concentrations of nitrates and phosphates. Farmers practice inorganic nutrient enrichment in the Philippines to increase growth (Tahiluddin et al., 2023). The positive effect of supplying nitrogen fertiliser was also demonstrated experimentally (Li

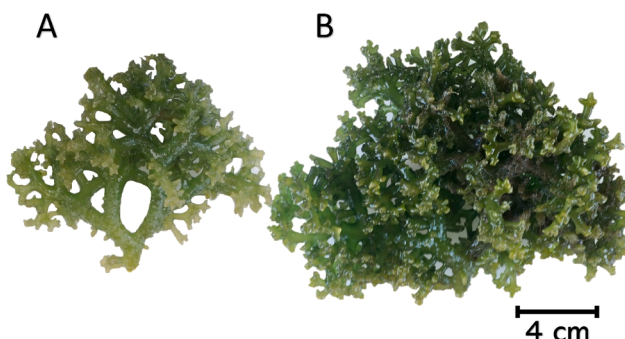


Fig. 3. Morphological and colour changes of a green morphotype of *K. alvarezii* during a cultivation cycle in Takalar Regency (South Sulawesi, Indonesia). A. Observation at t_{10} (26/10/2021). B. Observation of the same thallus at t_{40} (23/11/2021). The illumination conditions have been standardized using a common white background.

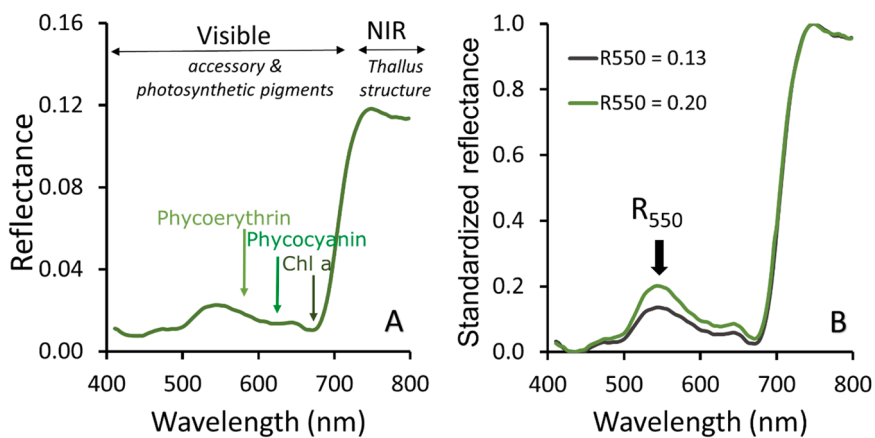


Fig. 4. A. Spectral signature of *K. alvarezii* measured by spectroradiometry, showing light absorption by photosynthetically active pigments (Carotenoids, Phycoerythrin, Phycocyanin, Chlorophyll-a) in the visible wavelength range and a characteristic reflection in the near-infrared (NIR) related to the structure of the thallus (Davies et al. 2023). The wavelengths corresponding to the absorption bands of the pigments were obtained from Kumar et al. (2020). (B) The Greenness index at R_{550} is estimated from standardized reflectance. The two reflectance spectra correspond to a greener seaweed ($R_{550} = 0.20$) compared to a darker one, less green ($R_{550} = 0.13$).

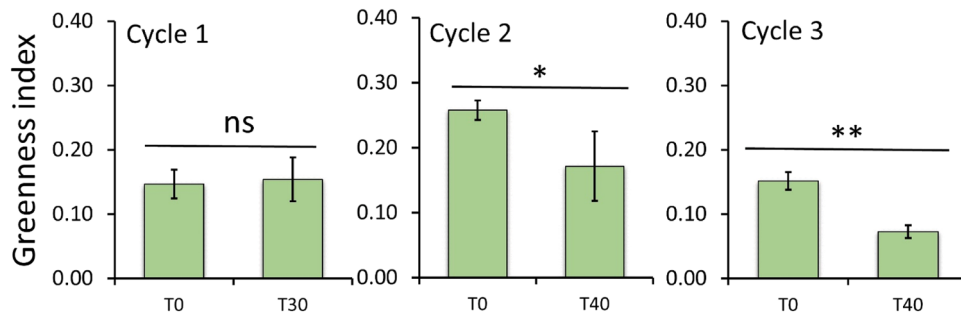


Fig. 5. Changes in the Greenness index of *K. alvarezii* over time during three cultivation cycles from July to November 2021 in South Sulawesi (Indonesia). Cycles 1 & 2 correspond to the dry season and Cycle 3 to the wet season; $n = 9$, * denotes statistical difference $p < 0.05$ ** denotes high statistical difference $p < 0.01$. ns = no statistical difference.

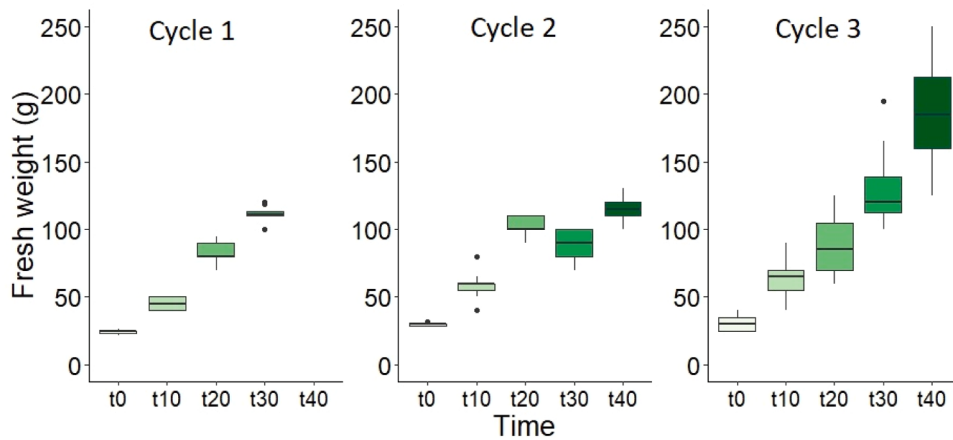


Fig. 6. Changes in median fresh weight (g) of *K. alvarezii* during three cultivation cycles from July to November 2021 in South Sulawesi (Indonesia). Cycles 1 and 2 correspond to the dry season and Cycle 3 to the wet season, $n = 9$.

et al., 1990). However, these authors also showed that ammonium concentrations higher than 35 mM ($0.63 \text{ mg.L}^{-1} \text{ NH}_4^+$) had a negative effect on growth. There is an upper limit to the nutrient concentrations, and polluted eutrophic waters are likely unfavourable. The comparison with nutrient concentration from other studies should be made cautiously, as there is an interaction with the water flow, facilitating their absorption (Hurd, 2000). However, it would be helpful to assess

the sub-optimal concentrations, which may be related to carrying capacity issues reported by farmers (Zamroni and Yamao, 2011). Regional and even idiosyncratic local conditions can mask seasonal variations of nutrients, for example, when a seaweed cultivation area receives effluents from a shrimp farm. Neish (2013) reported that in some locations, farmers from South Sulawesi described the dry season as best for production, a statement that was contrary to the result of this study. To

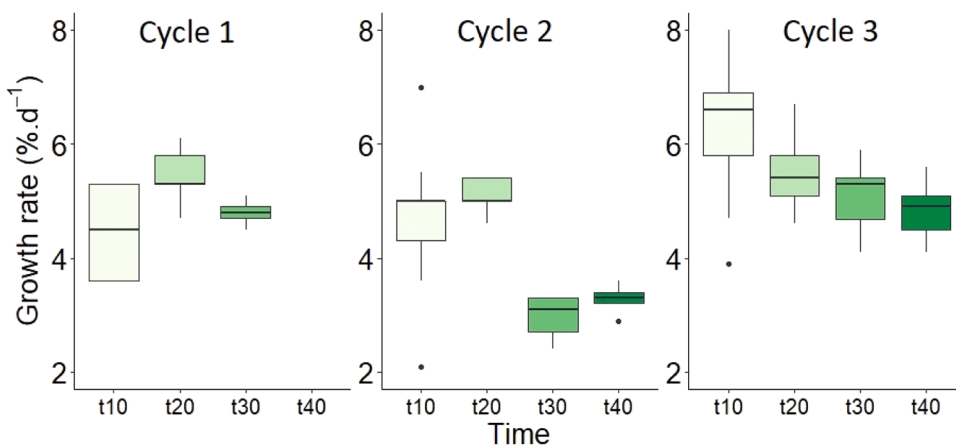


Fig. 7. Changes in median Specific Growth Rate (%.day^{-1}) of *K. alvarezii* during three cultivation cycles from July to November 2021 in South Sulawesi (Indonesia). Cycles 1 and 2 correspond to the dry season and Cycle 3 to the wet season, $n = 9$.

Table 2

Spearman correlations between *K. alvarezii* SGR (%.d^{-1}) and environmental variables: pH, turbidity (NTU), nitrate (NO_3^-), phosphate (PO_4^{3-}), salinity (PSU), and temperature (Temp, $^{\circ}\text{C}$). * indicates $p < 0.05$, ** indicates $p < 0.01$ and ns indicates not significant $p > 0.05$.

SGR	pH	NTU	Nitrate	Phosphate	Salinity	Temp
SGR	-0.33**	0.11 ns	0.12 ns	0.21 **	-0.35 **	0.14 ns
pH		-0.26*	-0.16 ns	-0.17 ns	0.70**	-0.56**
NTU			0.01 ns	0.39**	-0.26**	0.23*
Nitrate				0.23*	-0.42**	0.13 ns
Phosphate					-0.34**	0.26*
Salinity						-0.51**
Temp						

clarify such contradictory observations and establish causal relationships, there is a need for water quality monitoring, in particular, nutrients collected during seasonal cycles, to obtain a broader range of variations. It is also essential to disentangle genetics from the environmental source of variations in growth and production (Simatupang et al., 2021). From an operational perspective, this seasonal variability is pushing the farmers to change cultivation sites and cultivars or even to use the less valued, but more resistant *Eucheuma denticulatum* (Ward et al., 2021), as was the case in 2023 in Punaga (Barillé, pers. comm.). These are strong constraints for the farmers (Cai et al., 2013). Understanding causal mechanisms related to seasonal growth variations and seaweed health could help provide an early warning (Mateo et al., 2020).

4.2. Seasonal changes in growth and production

The highest growth rate of $5.0\text{ \%}\cdot\text{day}^{-1}$ at harvest (t_{40}) was estimated for Cycle 3 during the West monsoon season. In contrast, a value of $2.4\text{ \%}\cdot\text{day}^{-1}$ was previously reported by Kasim and Mustafa (2017) and $6.0\text{ \%}\cdot\text{day}^{-1}$ by Febriyanti et al. (2019) in Sulawesi. In this study, the most pronounced difference in SGR was after ten days of cultivation (t_{10}), with 6.6 \% day^{-1} for Cycle 3 vs. 4.5 \% day^{-1} and 5.2 \% day^{-1} for Cycle 1 and 2, respectively. Overall, the SGR decreased during cycles from t_{10} to t_{40} in coherence with the general principle of allometric growth (Stagnol et al., 2016). The lowest SGR of $3.3\text{ \%}\cdot\text{day}^{-1}$ at harvest (t_{40}) estimated for Cycle 2 can be partly explained by a loss of biomass between t_{20} and t_{30} due to strong waves. Although no replicates were lost, some branches of the thallus were broken. Hydrodynamism is another significant environmental abiotic variable, particularly in shallow areas, as was the case for the cultivation plots of this study. Farmers anticipate adverse hydrodynamic conditions and harvest early to avoid losing seaweed or even lines (Zamroni and Yamao, 2011). This was the case for Cycle 1, when the seaweed was harvested after 30 days.

This explains the low production of 484.4 g.m^{-1} for Cycle 1. The highest production of 827.8 g.m^{-1} was recorded for Cycle 3 during the West monsoon. This falls, however, in the lower range of values reported by Simatupang et al. (2021) for Indonesia, with their best sites of Bontang and Kupang having a production higher than 2000 g.m^{-1} . The methodology in this study is not strictly comparable to assessing production rates (weighing complete lines vs. individual thallus). Still, interestingly, they observed a large variability, with the poorest growing location producing only 495 g.m^{-1} . However, there was no relationship between production and carrageenan content, gel strength and viscosity. The highest product quality was measured for the lowest production sites (Simatupang et al., 2021). Future studies on growth and production should ideally combine measurements of seaweed quality, a high-frequency monitoring of relevant environmental variables and a genetic characterisation of the cultivars. Variability in growth and production is inherently multifactorial and complex. Still, three main factors can be considered in the first approach (Simatupang et al., 2021): the culture methods, the genetic diversity and the environment. This study used the same long-line method during the three cycles. Therefore, the variability related to a different cultural technique (Hayashi et al., 2010, Kasim and Mustafa, 2017) was discarded. The farmer who cultivated the seaweed during the three cycles was producing and using his cultivar of the green morphotype of *K. alvarezii*. We, therefore, hypothesised that the genetic factor was not the leading cause of the observed seasonal growth and production variation. At the level of the Indonesian archipelago, Ratnawati et al. (2020) showed a limited genetic diversity of farmed *Kappaphycus*. However, there was no molecular quantification of the genetic distance between cultivars used for each cycle. There is a large phenotypic plasticity in cultivated *K. alvarezii* (Tan et al., 2017; Simatupang et al., 2021). The cultivar used in this study had the same morphology and green colour throughout the monsoon seasons (Fig. 3), although greenness variations were quantified by spectroradiometry. For the above reasons, the environment, specifically abiotic

variables, was likely the main driving factor of seasonal growth and production changes.

4.3. Colour variations

K. alvareezi green morphotype's spectral signature (Fig. 4), was similar to green macrophyte spectra (Davies et al., 2023). It reflects more light in the green spectral region 500–600 nm, and the greenness of the seaweed was quantified in this study using an optical index at 550 nm. *K. alvarezii* has many colour morphotypes around three main chroma: green, brown and red (Hayashi et al., 2010; Tan et al., 2017). The colour of this seaweed is related to its pigment composition, which absorbs light in the visible wavelength domain. As for all photosynthetic plants, the main pigment of *K. alvarezii* is chlorophyll *a*, but it possesses the characteristic pigments of a rhodophyte: phycoerythrin, phycocyanin and allophycocyanin (Kumar et al., 2020). Phycoerythrin is lower in the green morphotype (Dawes, 1992), but Aguirre-von-Wobeser et al. (2001) have also shown that there was an overexpression of phycocyanin and allophycocyanin masking the red colour. Spectral reflectance has been recently used to discriminate seaweed morphotypes (Fidai et al., 2024). In this study, we observed a darkening of the seaweed at the end of the cultivation period for two cycles of the dry and wet seasons. The lack of significant difference for Cycle 1 could be related to the shorter duration. The thalli appeared dark green compared to the greener colouration of the seedlings. Li et al. (1990) observed a darkening of the thallus colour following nitrogen fertilisation. This would be consistent with the higher nitrate concentrations measured for Cycle 3 during the West monsoon season. Still, this colour change was also observed during Cycle 2, when nutrients had lower concentrations. We cannot exclude that the darkening was related to increased pigment concentrations that would absorb more light in the visible wavelength range. Seasonal variations of pigment concentrations concerning light availability are a known phenomenon for marine macrophytes (Bargain et al., 2013). The cultivar used in Cycle 2 was greener than the others, suggesting a higher proportion of phycocyanin and allophycocyanin. These variations could be related to photoprotection mechanisms to reduce photodamage after photoinhibition (Aguirre-von-Wobeser et al., 2001). An experimental approach combining light and nitrogen concentration would help elucidate the determinism of colour changes concerning these two environmental variables. The objective of quantifying seaweed colour changes with spectral reflectance is to develop optical health indices as they already exist in agriculture (Meng et al., 2020). For *K. alvarezii*, the method could also be used to discriminate the different morphotypes based on their colour and the internal structure of the thallus. In angiosperms, the spectral features in the near-infrared regions have long been known to be related to the structure of the tissues (Slaton et al., 2001). For *K. alvarezii*, it could be related to cortex and medullar tissues and their eventual disruption, but this was not investigated in this study. At longer wavelengths of shortwave infrared (ca. 1000–2500 nm), the reflectance bears information on the biochemical composition (Fidai et al., 2024). *In situ*, we observed that other factors could influence colour than pigments, such as epiphytes, sedimentation on the thallus, and whitening due to the ice-ice disease. Epiphytes are a major concern for eucheumatoid aquaculture (e.g., Hayashi et al., 2010, 2017; Hurtado et al., 2006; Vairappan, 2006). In this study, the green morphotypes were colonised by very few filamentous rhodophytes, and the main biofoulers were small bryozoans. Epiphytes and herbivorous fish were not reported as an issue by the farmers. This overall low epiphyte presence could be related to the turbidity of the area, as thalli were often covered with sediment. However, the farmers were shaking the lines daily to eliminate sediment and debris, a higher frequency than previously reported (Mateo et al., 2020; Tahiluddin et al., 2023). The ice-ice symptoms of thallus whitening were only observed in Cycle 3 during the wet West monsoon season, and several replicates were lost. It corresponded with a critical shift in abiotic variables with a rise in temperature and a decrease in salinity, as

in many recorded incidences of ice-ice disease (Ward et al., 2021). While whitening could be observed in the cultivation plots, the replicates were not discoloured. The ten-day interval was likely too long to detect the temporal dynamic of discolouration, and we suggest daily spectral measurements. The spectral shape of a white thallus has a flat and relatively uniform spectral reflectance across the visible spectrum (not shown), corresponding to a loss of photosynthetic and accessory pigments (Ganzon-Fortes et al., 1993). It is very different from the spectrum of a healthy green morphotype. The percent cover of partial discolouration from which the whitening can be detected has been investigated (Alevizos et al., 2024). An important perspective of this spectral characterisation of colour is the potential for remote sensing by drones to capture variations at the scale of cultivation plots (Nurdin et al., 2023), offering farmers tools for early warning of crop and yield conditions. Optical indices can indeed be upscaled to drone sensors, opening the way to high-resolution seaweed aquaculture mapping.

5. Conclusion

In this work, colour changes in *K. alvarezii* were quantified using spectral reflectance, with thalli getting darker at the end of cultivation cycles. Spectroradiometry has a long history in agriculture but has rarely been applied to aquaculture. It has been used to discriminate *Sargassum* sp. morphotypes, which could be tested for eucheumatoids. Optical health indices could be developed whenever colour is involved, such as the whitening of the thallus for the ice-ice or the presence of red epiphytes. We also showed a striking environmental shift between the East and West monsoons. The best growth and production were obtained during the wet West monsoon, with higher nutrients and temperature but lower salinity. Paradoxically, it was also the season when the ice-ice disease was observed for the first time, with a higher risk for farmers. The amount and frequency of rainfall are likely key factors. Our work combined with farmers feedbacks suggest that an alteration of the West monsoon rainfall can impact the growth of *K. alvarezii* in South Sulawesi. In 2023, the farmers reported that they could not grow the green morphotype from September to November because of a lack of rain and shifted for the more resistant but less valued *Eucheuma denticulatum* (Barillé pers. comm.). Selecting strains of the green morphotype of *K. alvarezii* should be prioritized to develop a cultivar better adapted to these shifting environmental conditions.

CRediT authorship contribution statement

Elisabeth J. Cook-Cottier: Writing – review & editing, Validation, Supervision. **Nurjannah Nurdin:** Supervision, Resources, Methodology, Investigation, Funding acquisition, Formal analysis, Conceptualization. **Agus Aris:** Software, Investigation, Data curation. **Iona L.R. Paterson:** Writing – review & editing, Writing – original draft, Methodology, Investigation. **Simo Oiry:** Writing – review & editing, Software, Formal analysis, Data curation. **Laurent Barillé:** Writing – review & editing, Writing – original draft, Project administration, Methodology, Funding acquisition, Formal analysis, Conceptualization.

Author agreement statement

We the undersigned declare that this manuscript is original, has not been published before and is not currently being considered for publication elsewhere.

We confirm that the manuscript has been read and approved by all named authors and that there are no other persons who satisfied the criteria for authorship but are not listed. We further confirm that the order of authors listed in the manuscript has been approved by all of us.

We understand that the Corresponding Author is the sole contact for the Editorial process. He/she is responsible for communicating with the other authors about progress, submissions of revisions and final approval of proofs

On behalf of all co-authors,

Declaration of Competing Interest

The authors declare that they have no known competing financial interests or personal relationships that could have appeared to influence the work reported in this paper.

Acknowledgements

This work was partially supported by the "PHC NUSANTARA" program (project number: 47060PG), funded by the French Ministry for Europe and Foreign Affairs, the French Ministry for Higher Education and Research and the Ministry of Education & Culture, Riset & Technology of Indonesia (partner). This work received additional funding by the LPPM Hasanuddin University through the Scheme of International Collaboration Research (ICORE) 2023. Grant Number 04966/UN4.22/PT.01.03/2023. I.P. was supported by the Erasmus+: Key Action 1 – Erasmus Mundus Joint Master Degrees (EMJMD) (Grant No. 599111-EPP-1-2018-1-EL-EPPKA1-JMD-MOB) for the EMJMD in Aquaculture, Environment and Society PLUS (ACES+). We want to thank Evangelos Alevizos for helping with the NASA and Copernicus data.

Data availability

Data will be made available on request.

References

- Aguirre-von-Wobeser, E., Figueiroa, F., Cabello-Pasini, A., 2001. Photosynthesis and growth of red and green morphotypes of *Kappaphycus alvarezii* (Rhodophyta) from the Philippines. Mar. Biol. 138, 679–686. <https://doi.org/10.1007/s002270000506>.
- Alevizos, E., Nurdin, N., Aris, A., Barillé, L., 2024. Proximal sensing for characterising seaweed aquaculture crop: optical detection of ice-ice disease. Remote Sens. 16, 3502. <https://doi.org/10.3390/rs16183502>.
- Ambo-Rappe, R., Moore, A.M., 2018. Sulawesi seas, Indonesia. World Seas: An Environmental Evaluation Volume II: The Indian Ocean to the Pacific. Elsevier, pp. 559–581. <https://doi.org/10.1016/B978-0-08-100853-9.00032-4>.
- Aslan, L.M., 1998. Seaweed Cultivation (Rumput Laut). Kanisius, Yogyakarta, 97p.
- Anzola, R.V., Ask, E., 2017. In: Hurtado, A., Critchley, A., Neish, I. (Eds.), Tropical Seaweed Farming Trends, Problems and Opportunities: Developments in Applied Phycology, Reproductive biology and eco-physiology of farmed kappaphycus and eucheuma, 9. Springer, Cham. https://doi.org/10.1007/978-3-319-63498-2_3.
- Bargain, A., Robin, M., Méléder, V., Rosa, P., Le Menn, E., Harin, N., Barillé, L., 2013. Seasonal spectral variation of *Zostera noltii* and its influence on pigment-based Vegetation Indices. J. Exp. Mar. Biol. Ecol. 446, 86–94. <https://doi.org/10.1016/j.jembe.2013.04.012>.
- Brakel, J., Sibonga, R., Dumilag, R.V., Montalecot, V., Campbell, I., Cottier-Cook, E.J., Ward, G., Le Masson, V., Liu, T., Msuya, F.E., Brodie, J., Lim, P.E., Gachon, C.M.M., 2021. Exploring, harnessing, and conserving genetic resources towards a sustainable seaweed aquaculture. Plants People Planet 3 (4), 337–349. <https://doi.org/10.1002/ppp3.10190>.
- Cai, J., Hishamunda, N., Ridler, N., 2013. Social and economic dimensions of carrageenan seaweed farming: a global synthesis. In: Valderrama, D., Cai, J., Hishamunda, N., Ridler, N. (Eds.), Social and Economic Dimensions of Carrageenan Seaweed Farming, Fisheries and Aquaculture Technical Paper No, 580. FAO, Rome, pp. 5–59.
- Cao, F., Yang, Z., Ren, J., Jiang, M., Ling, W.K., 2017. Does Normalization Methods Play a Role for Hyperspectral Image Classification? 2–7. arXiv:1710.02939.
- R Core Team, 2022. R: A Language and Environment for Statistical Computing. RFoundation for Statistical Computing, Vienna, Austria.
- Cottier-Cook, E.J., Nagabhatla, N., Asri, A., Beveridge, M., Bianchi, P., Bolton, J., Bondad-Reantaso, M.G., Brodie, J., Buschmann, A., Cabarubias, J., Campbell, I., Chopin, T., Critchley, A., De Lombaerde, P., Doumeizel, V., Gachon, C.M.M., Hayashi, L., Hewitt, C.L., Huang, J., Hurtado, A.Q., Kambez, C., Kim, G.H., Le Masson, V., Lim, P.E., Liu, T., Malin, G., Matoju, I., Montalecot, V., Msuya, F.E., Potin, P., Puspita, M., Qi, Z., Shaxson, L., Sousa Pinto, I., Stentiford, G.D., Suyo, J., Yarish, C., 2021. Ensuring the Sustainable Future of the Rapidly Expanding Global Seaweed Aquaculture Industry – A Vision. United Nations University Institute on Comparative Regional Integration Studies and Scottish Association for Marine Science Policy Brief. ISBN 978-92-808-9135-5.
- Davies, B.F.R., Gernez, P., Geraud, A., Oiry, S., Rosa, P., Zoffoli, M.L., Barillé, L., 2023. Multi- and hyperspectral classification of soft-bottom intertidal vegetation using a spectral library for coastal biodiversity remote sensing. Remote Sens. Environ. 290, 113554. <https://doi.org/10.1016/j.rse.2023.113554>.
- Dawes, C.J., 1992. Irradiance acclimation of the cultured Philippine seaweeds, *Kappaphycus alvarezii* and *Eucheuma denticulatum*. Bot. Mar. 35 (3). <https://doi.org/10.1515/botm.1992.35.3.189>.
- Douay, F., Verpoorter, C., Duong, G., Spilmont, N., Gevaert, F., 2022. New Hyperspectral Procedure to Discriminate Intertidal Macroalgae. Remote Sens. 14. <https://doi.org/10.3390/rs14020346>.
- FAO. 2022. The State of World Fisheries and Aquaculture 2022. Towards Blue Transformation. Rome, FAO. <https://doi.org/10.4060/cc0461en>.
- FAO. 2024. The State of World Fisheries and Aquaculture 2024. Blue Transformation in Action. Rome, FAO. <https://doi.org/10.4060/cd0683en>.
- Febriyanti, F., Aslan, L.O.M., Iba, W., Patadhai, A.B., Nurdin, A.R., 2019. Effect of Various Planting Distances on Growth and Carrageenan Yield of *Kappaphycus alvarezii* (Doty) Using Seedlings Produced from Mass Selection Combined with Tissue-cultured Method. IOP Conf. Ser. Earth Environ. Sci. 2019278012027.
- Ferdouse, F., Lovstad, Holdt, S., Smith, R., Muria, P., Yang, Z., 2018. The global status of seaweed production, trade and utilization. FAO Globefish Res. Program. 124, 120.
- Fidai, Y.A., Botelho Machado, C., Dominguez Amela, V., Oxenford, H.A., Jayson-Quashigah, P.-N., Tonon, T., Dash, J., 2024. Innovative spectral characterization of beached pelagic sargassum towards remote estimation of biochemical and phenotypic properties. Sci. Total Environ. 914, 169789. <https://doi.org/10.1016/j.scitotenv.2023.169789>.
- Ganzon-Fortes, E.T., Azanza-Corrales, R., Aliaza, T., 1993. Comparison of photosynthetic responses of healthy and 'Diseased' *Kappaphycus alvarezii* (Doty) Doty using P vs I curve. Bot. Mar. 36 (6), 503–506. <https://doi.org/10.1515/botm.1993.36.6.503>.
- Gitelson, A.A., Merzlyak, M.N., 1996. Signature analysis of leaf reflectance spectra: algorithm development for remote sensing of chlorophyll. J. Plant Physiol. 148, 494–500. [https://doi.org/10.1016/S0176-1617\(96\)80284-7](https://doi.org/10.1016/S0176-1617(96)80284-7).
- Gordon, A.L., Napitu, A., Huber, B.A., Gruenberg, L.K., Pujiana, K., Agustiadi, T., Kuswardani, A., Mbay, N., Setiawan, A., 2019. Makassar strait throughflow seasonal and interannual variability, an overview. J. Geo. Res. Oceans. <https://doi.org/10.1029/2018JC014502>.
- Hayashi, L., Hurtado, A.Q., Msuya, F.E., Bleicher-Lhoneur, G., Critchley, A.T., 2010. A Review of *Kappaphycus* Farming: Prospects and Constraints. In: Seckbach, J., Einav, R., Israel, A. (Eds.), Seaweeds and their role in globally changing environments, 2010. Springer, Dordrecht, pp. 251–283.
- Hayashi, L., Reis, R.P., dos Santos, A.A., Castellar, B., Robledo, D., de Vega, G.B., Msuya, F.E., Eswaran, K., Yasir, S.M.D., Ali, M.K.M., Hurtado, A.Q., 2017. The Cultivation of *Kappaphycus* and *Eucheuma* in Tropical and Sub-tropical Waters. In: Tropical Seaweed Farming Trends, Problems and Opportunities: Focus on *Kappaphycus* and *Eucheuma* of Commerce; Developments in Applied Phycology; Hurtado, A.Q., Critchley, A.T., Neish, I.C., Eds.; Springer: Cham, Switzerland, 2 pp. 55–90. ISBN 978-3-319-63498-2.
- Hidayat, R., Junianti, M.D., Ma'rufah, U., 2017. Impact of La Niña and La Niña Modoki on Indonesia rainfall variability. IOP Conf. Ser.: Earth Environ. Sci. 149012046 doi: 10.1088/1755-1315/149/1/012046.
- Hung, L.D., Hori, K., Nang, H.Q., Kha, T., Hoa, L.T., 2009. 2009. Seasonal changes in growth rate, carrageenan yield and lectin content in the red alga *Kappaphycus alvarezii* cultivated in Camranh Bay, Vietnam. J. Appl. Phycol. 21, 265–272. <https://doi.org/10.1007/s10811-008-9360-2>.
- Hurd, C.L., 2000. Water motion, marine macroalgal physiology, and production. J. Phycol. 36 (3), 453–472.
- Hurtado, A., Critchley, A., Neish, I., 2017. Tropical Seaweed Farming Trends, Problems and Opportunities. Developments in Applied Phycology, 9. Springer, Cham. https://doi.org/10.1007/978-3-319-63498-2_3.
- Hurtado, A.Q., Critchley, A.T., Trespoey, A., Lhoneur, G.B., 2006. Occurrence of *Polysiphonia* epiphytes in *Kappaphycus* farms at Calaguas Is., Camarines Norte, Philippines. J. Appl. Phycol. 18, 301–306. <https://doi.org/10.1007/s10811-006-9032-z>.
- Hurtado, A.Q., Gerung, G.S., Yasir, S., Critchley, A.T., 2014. Cultivation of tropical red seaweeds in the BIMP-EAGA region. J. Appl. Phycol. 26, 707–718. <https://doi.org/10.1007/s10811-013-0116-2>.
- Janßen, A., Wizemann, A., Klippera, A., Satari, D.Y., Westphal, H., Mann, T., 2017. Sediment composition and facies of coral reef Islands in the Spermonde Archipelago, Indonesia. Front. Mar. Sci. 17. <https://doi.org/10.3389/fmars.2017.00144>.
- Kambey, C.S.B., Campbell, I., Cottier-Cook, E.J., Nor, A.R.M., Kassim, A., Sade, A., Lim, P.E., 2021. Seaweed aquaculture: a preliminary assessment of biosecurity measures for controlling the ice-ice syndrome and pest outbreaks of a *Kappaphycus* farm. J. Appl. Phycol. 33, 3179–3197. <https://doi.org/10.1007/s10811-021-02530-z>.
- Kasim, M., Mustafa, A., 2017. Comparison growth of *Kappaphycus alvarezii* (Rhodophyta, Solieriaceae) cultivation in floating cage and longline in Indonesia. Aquac. Rep. 6, 49–55. <https://doi.org/10.1016/j.agrep.2017.03.004>.
- Kotiya, A.S., Gunalan, B., Parmar, H.V., M, J., Tushar, D., Solanki, J.B., Makwana, N.P., 2011. Growth comparison of the seaweed *Kappaphycus alvarezii* in nine different coastal areas of Gujarat coast, India. Adv. Appl. Sci. Res. 2, 99–106.
- Kumar, S., Ganeshan, K., Subba Rao, P.V., 2014. Seasonal variation in nutritional composition of *Kappaphycus alvarezii* (Doty) Doty—an edible seaweed. J. Food Sci. Technol. 52, 2751–2760. <https://doi.org/10.1007/s13197-014-1372-0>.
- Kumar, Y.N., Poong, S.-W., Gachon, C., Brodie, J., Sade, A., Lim, P.-E., 2020. Impact of elevated temperature on the physiological and biochemical responses of *Kappaphycus alvarezii* (Rhodophyta). PLoS ONE 15 (9), e0239097. <https://doi.org/10.1371/journal.pone.0239097>.
- Largo, D.B., Fukami, K., Nishijima, T., 1995a. Occasional pathogenic bacteria promoting ice-ice disease in the carrageenan-producing red algae *Kappaphycus alvarezii* and *Eucheuma denticulatum* (Solieriaceae, Gigartinales, Rhodophyta). J. Appl. Phycol. 7, 545–554.

- Largo, D.B., Fukami, K., Nishijima, T., Ohno, M., 1995b. Laboratory-induced development of the ice-ice disease of the farmed red algae *Kappaphycus alvarezii* and *Eucheuma denticulatum* (Solieriaceae, Gigartinales, Rhodophyta). *J. Appl. Phycol.* 7, 539–543.
- Li, R., Li, J., Wu, C.Y., 1990. Effect of ammonium on growth and carrageenan content in *Kappaphycus alvarezii* (Gigartinales, Rhodophyta). *Hydrobiologia* 249–503.
- Lo, Y.Y., Billia, L., Singh, A., 2015. Effect of climate change on seasonal monsoon in Asia and its impact on the variability of monsoon rainfall in Southeast Asia. *Geosci. Front.* 6 (6), 817–823. <https://doi.org/10.1016/j.gsf.2014.02.009>.
- Mandal, S.K., Ajay, G., Monisha, N., Malarvizhi, J., Temkar, G., Mantri, V.A., 2014. Differential response of varying temperature and salinity regimes on nutrient uptake of drifting fragments of *Kappaphycus alvarezii*: implication on survival and growth. *J. Appl. Phycol.* 27 (2015), 1571–1581. <https://doi.org/10.1007/s10811-014-0469-1>.
- Mateo, J.P., Campbell, I., Cottier-Cook, E.J., Luhan, M.R.J., Ferriols, V.M.E.N., Hurtado, A.Q., 2020. Analysis of biosecurity-related policies governing the seaweed industry in the Philippines. *J. Appl. Phycol.* 32, 2009–2022. (<https://link.springer.com/article/10.1007%2Fs10811-020-02083-7>).
- Mayer, B., Damm, P.E., 2012. The Makassar Strait throughflow and its jet. *J. Geo. Res.* 117. <https://doi.org/10.1029/2011JC007809>. C07020.
- Meng, R., Lv, Z., Yan, J., Chen, G., Zhao, F., Zen, L., Xu, B., 2020. Development of spectral disease indices for southern corn rust detection and severity classification. *Remote Sens.* 12, 1–16. <https://doi.org/10.3390/rs12193233>.
- Msuya, F.E., Porter, M., 2014. Impact of environmental changes on farmed seaweed and farmers: the case of Songo Songo Island, Tanzania. *J. Appl. Phycol.* 26, 2135–2141. <https://doi.org/10.1007/s10811-014-0243-4>.
- Ndawala, M.A., Msuya, F.E., Cabarubias, J.P., Kambez, C.S.B., Buriyo, A., Mvungi, E., Cottier-Cook, E.J., 2022. Effect of biosecurity practices and diseases on growth and carrageenan properties of *Kappaphycus alvarezii* and *Eucheuma denticulatum* cultivated in Zanzibar, Tanzania. *J. Appl. Phycol.* 34, 3069–3085. <https://doi.org/10.1007/s10811-022-02835-7>.
- Neish, I.C., 2013. Social and Economic Dimensions of Carrageenan Seaweed Farming in Indonesia. In: D., Valderrama, J., Cai, N., Hishamunda and N., Ridler, eds. Social and economic dimensions of carrageenan seaweed farming. Fisheries and Aquaculture Technical Paper No. 580. 61–89..
- Neish, I.C., Sepulveda, M., Hurtado, A.Q., Critchley, A.T., 2017. Reflections on the Commercial Development of Eucheumatoid Seaweed Farming. *Trop. Seaweed Farming Trends Probl.* Oppor. 1–27. https://doi.org/10.1007/978-3-319-63498-2_1.
- Nurdin, N., Alevizos, E., Syamsuddin, R., Asis, H., Zainuddin, E.N., Aris, A., Oiry, S., Brunier, G., Komatsu, T., Barillé, L., 2023. Precision aquaculture drone mapping of the spatial distribution of *Kappaphycus alvarezii* biomass and Carrageenan. *Remote Sens.* 15, 3674. <https://doi.org/10.3390/rs15143674>.
- Nuryartono, N., Waldron, S., Tarman, K., Siregar, U., Pasaribu, S., Langford, A., Farid, M., Sulfaahri, 2021. An analysis of the South Sulawesi seaweed industry. *Aust. Indones. Cent. Tech. Rep.* 25. <https://doi.org/10.13140/RG.2.2.13785.24169>.
- Ratnawati, P., Simatupang, N.F., Pong-Masak, P.R., Paul, N.A., Zuccarello, G.C., 2020. Genetic diversity analysis of cultivated *Kappaphycus* in Indonesian seaweed farms using COI gene. *Squalen. Bull. Mar. Fish. Postharvest Biotechnol.* 15, 65–72.
- Rimmer, M.A., Larson, S., Lapong, I., Purnomo, A.H., Pong-masak, P.R., Swanepoel, L., Paul, N.A., 2021. Seaweed aquaculture in Indonesia contributes to social and economic aspects of livelihoods and community wellbeing. *Sustainability*. <https://doi.org/10.3390/su131910946>.
- Setyawidati, N., Liabot, P.O., Perrot, T., Radiarta, N., Deslandes, E., Bourgougnon, N., Rossi, N., Stiger-Pouvreau, V., 2017. *In situ* variability of carrageenan content and biomass in the cultivated red macroalgae *Kappaphycus alvarezii* with an estimation of its carrageenan stock at the scale of the Malasoro Bay (Indonesia) using satellite image processing. *J. Appl. Phycol.* 2307–2321. <https://doi.org/10.1007/s10811-017-1200-9>.
- Simatupang, N.F., Pong-Masak, P.R., Ratnawati, P., Agusman, Paul, N.A., Rimmer, M.A., 2021. Growth and product quality of the seaweed *Kappaphycus alvarezii* from different farming locations in Indonesia. *Aquac. Rep.* 20. <https://doi.org/10.1016/j.aqrep.2021.100685>.
- Slaton, M.R., Hunt, E.R., Smith, W.K., 2001. Estimating near-infrared leaf reflectance from leaf structural characteristics. *Am. J. Bot.* 88 (2), 278–284. <https://doi.org/10.2307/2657019>.
- Stagnol, D., Macé, M., Destombe, C., Davoult, D., 2016. Allometric relationships for intertidal macroalgae species of commercial interest. *J. Appl. Phycol.* 1–5. <https://doi.org/10.1007/s10811-016-0860-1>.
- Strickland, J.D.H., Parsons, T.R., 1972. *A Practical Handbook of Seawater analysis. Fisheries Research Board of Canada*, Ottawa.
- Tahiluddin, A.B., Imbuk, E.S., Sarri, J.H., Mohammad, H.S., Ensano, F.N.T., Maddan, M., M., Cabilin, B.S., 2023. Eucheumatoid seaweed farming in the southern Philippines. *Aquat. Bot.* 189, 103697. <https://doi.org/10.1016/j.aquabot.2023.103697>.
- Tan, J., Lim, P.E., Phang, S.M., Hurtado, A.Q., 2017. Biodiversity, biogeography and molecular genetics of the commercially important genera *Kappaphycus* and *Eucheuma*. In: Hurtado, A., Critchley, A., Neish, I. (Eds.), *Tropical Seaweed Farming Trends, Problems and Opportunities. Developments in Applied Phycology*, 9. Springer, Cham. https://doi.org/10.1007/978-3-319-63498-2_2.
- Vairappan, C.S., 2006. Seasonal occurrences of epiphytic algae on the commercially cultivated red alga *Kappaphycus alvarezii* (Solieriaceae, Gigartinales, Rhodophyta). *J. Appl. Phycol.* 18, 611–617. <https://doi.org/10.1007/s10811-006-9062-6>.
- Vairappan, C.S., Chung, C.S., Hurtado, A.Q., Soya, F.E., Lhonneur, G.B., Critchley, A., 2008. Distribution and symptoms of epiphyte infection in major carrageenophyte-producing farms. *J. Appl. Phycol.* 20, 477–483. <https://doi.org/10.1007/s10811-007-9299-8>.
- Ward, G.M., Kambez, C.S.B., Faisan, J.P.Jr, Tan, P.-L., Daumich, C.C., Matouji, I., Stentiford, G.D., Bass, D., Lim, P.-E., Brodie, J., Poong, S.-W., 2021. Ice-Ice disease: an environmentally and microbiologically driven syndrome in tropical seaweed aquaculture. *Rev. Aquac.* 14, 414–439. <https://doi.org/10.1111/raq.12606>.
- Zamroni, A., Yamao, M., 2011. Coastal resource management: fishermen's perception of seaweed farming in Indonesia. *World Acad. Sci. Eng. Technol.* 60, 32–38.